THEORETICAL AND EXPERIMENTAL STUDY OF WATER VAPOUR CONDENSATION WITH HIGH CONTENT OF NON-CONDENSABLE GAS IN A VERTICAL TUBE

Jakub Krempaský*, Jan Havlík, Tomáš Dlouhý

Czech Technical University in Prague, Faculty of Mechanical Engineering, Department of Energy Engineering, Technická 4, Prague 6 16607, Czech Republic

* corresponding author: jakub.krempasky@fs.cvut.cz

ABSTRACT. This article deals with the possibility of separating water vapour from flue gases after oxyfuel combustion using condensation processes. Those processes can generally be described as condensation of water vapour in the presence of non-condensable gases. Hence, the effect of non-condensable gas (NCG) on the condensation process has been theoretically and experimentally analysed in this study. The theoretical model was developed on the basis of the heat and mass transfer analogy with respect to the effect of the NCG, the flow mode of the condensate film, the shear stress of the flowing mixture, subcooling and superheating. Subsequently, an experimental analysis was carried out on a 1.5 m long vertical pipe with an inner diameter of 23.7 mm. The mixture of vapour and air flowed inside the inner tube with an air mass fraction ranging from 23 % to 62 %. The overall heat transfer coefficients (HTC) from the theoretical model and experimental measurement are significantly lower than the HTC obtained according to the Nusselt theory for the condensation of pure water vapour. The overall HTC decreases along the tube length as the gas concentration increases, which corresponds to a decrease in the local condensation rate. The highest values of the HTC are observed in the condenser inlet, although a strong decrease in HTC is also observed here. Meanwhile, there is a possibility for an HTC enhancement through turbulence increase of the condensing mixture in the condenser outlet. Results also showed that the heat resistance of the mixture is several times higher than the heat resistance of the condensate film. The developed theoretical model based on heat and mass transfer analogy is in good agreement with experimental results with the standard deviation within +25 % and −5 %. The model is more accurate for lower NCG concentrations.

KEYWORDS: Condensation, non-condensable gas, vertical tube, experimental, theoretical.

1. INTRODUCTION

One of the promising CCS technologies is oxyfuel combustion. The use of CO_2 captured from oxyfuel combustion technology for other technological purposes and for storage requires a sufficient purity of the product. After emissions cleaning, suitable options for final drying of flue gases are condensation processes in condensing heat exchangers. The aim is to dry the flue gas formed by oxyfuel combustion, which is consists of steam and a high proportion of non-condensing gases (especially CO_2 and O_2). The drying is necessary for the final purification of CO2 prior to its further use. This process can generally be described as the condensation of water vapour with a high content of non-condensable gases.

Condensation of water vapour with the presence of non-condensable gas (e.g. CO_2) is a widely studied topic and its recognition dates back to 1873 [1]. Up to now, the main focus has been on condensation of water vapour with a small fraction of air in tube condensers [2, 3]. Such cases can be found in various technological processes such as refrigeration, condensers in power plants, geothermal power plants and various processes in chemical and process indus-

try. This field of study has been investigated by many authors and, today, represents a well-covered topic. However, there are areas where the content of air during the vapour condensation can be higher or different gas than air is present. For instance, it can be: CCU/S technologies, desalination of water, latent heat recovery from flue gas or LOCA accidents [2–4]. Therefore, studying condensation in tube condensers with respect to new technological challenges has a potential for commercial applications and system improvement.

Chantana [5] conducted an experimental and theoretical study of water vapour condensation in the presence of air in a vertical tube. The water vapour content in the gas vapour mixture was very low. The theoretical model was developed on the basis of the heat and mass transfer analogy. The results showed that the condensation of the vapour and roughness of the film surface cause a disruption of the gas layer accumulated near the phase interface, which increases the HTC. A detailed description of the processes at the vapour-liquid interface is also introduced in [6, 7]. Maheswari [8], in his work, studied the influence of the water vapour and air mixture's Reynolds number on the HTC in a vertical tube. He concluded that the

| Method | Semi-theoretical | | Theoretical | |
	Correction and degradation factor	Heat and mass transfer analogy	Diffusion layer model	Boundary layer model
Description	Empirical equations based on experimental data.	Based on similarities between momentum, energy, heat, and mass transfer equations and empirical coefficients.	Based on Fick's law of molecular diffusion. Vapour diffuses through the layer of non-condensable gas to phase interphase.	Description of condensate film layer and boundary layer with initial and boundary conditions.
Accuracy and output	Low accuracy, simple output.	Moderately high accuracy, usually iteration involved.	Moderately high accuracy, usually iteration involved.	High accuracy, various results, too complex for practical application.

TABLE 1. Overview of theoretical models for film-wise condensation with non-condensable gas.

HTC of the film can be lower than the HTC of the mixture in the case of high Reynolds number of the mixture. No and Park [9] conducted experiments in vertical and horizontal tubes. The most important observation was that the waviness of the film decreases the accumulation of gas near the phase interface, and thereby effectively increases heat transfer. The effect of gas velocity on the flow of the liquid film in the vertical tube is also studied in the work of the Kracik [10], where the effect of shear stress of the flowing gas on the liquid film is analysed experimentally and theoretically with three different diameters of the inner tube. Kuhn [11] created three theoretical models developed on degradation factor, heat and mass transfer analogy, and mass transfer modelling and compared them with results from an experimental measurement. The standard deviations of the HTC were 6.4 %, 8.4 % and 17.6 % for water vapour with air and 3.2 %, 6.1 % and 17.6 % for water vapour with helium according to the mass transfer modelling, diffusion layer modelling and degradation factor, respectively.

This article focuses on research of the process of condensation of water vapour from flue gases from oxyfuel combustion. In this study, the effect of non-condensable gas (NCG) on vapour condensation in a vertical tube condenser is theoretically and experimentally analysed.

2. THEORETICAL MODELLING

2.1. SUMMARY OF AVAILABLE THEORETICAL MODELS

There are several methods to calculate heat transfer during the condensation of water vapour in the presence of NCG in a vertical tube. In general, theoretical models for such phenomena are governed by the film condensation model, which was first described by Nusselt in 1916 [12]. Theoretical models based on the theory of film-wise condensation are usually divided into two groups, semi-theoretical and theoretical.

Semi-theoretical models use, to some extent, experimentally established coefficients and data, which are incorporated into the theoretical analysis. The first option is correction and degradation factors, which modify the standard theory for the condensation of pure vapour. The second option is models based on heat and mass transfer analogy. Meanwhile, theoretical models are not based on experimental data, but on the description of the boundary layer near the phase interphase. The general summary of the theoretical models is shown in Table 1 [3, 11, 13]. The degradation factor is the simplest method for the determination of HTC; however, it gives less accurate results. While the theoretical models are quite complex and can give very accurate results, their practical use is quite complicated.

2.2. DEVELOPED THEORETICAL MODEL

A theoretical model based on the heat and mass transfer analogy was developed for a vertical double-pipe condenser in which the condensing water vapour flows downwards in the inner tube and the cooling water flows in counter-current in the outer tube. Detailed descriptions of semi-theoretical models based on heat and mass transfer analogy can be found in the literature [5, 14, 15]. Herein, the condenser was divided into 15 segments where local heat transfer was determined. The overall HTC in the condenser is given by the heat transfer coefficients of several layers as shown in Figure 1 and described with Equation (1). One segment is shown in Figure 2.

Heat transfer of the condenser can be determined by a temperature difference and a corresponding HTC of the certain layer. The overall condenser power can be calculated from the temperature difference of bulk mixture temperature T_{SAT} and cooling water temperature T_K with the overall HTC of the condenser K. The heat transfer from the condensing mixture to the phase interface is given by the temperature difference of the bulk mixture T_{SAT} and phase interface $T_{F,SAT}$ and HTC of condensing mixture $\ddot{\alpha_G}$. This is equal
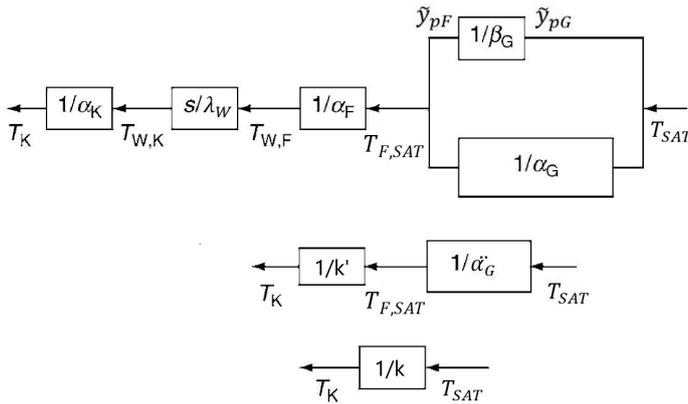
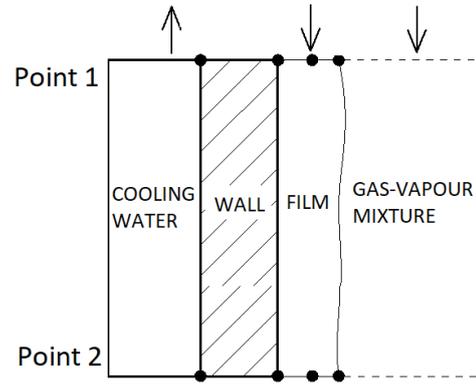FIGURE 1. Heat and mass resistances during condensation [14].

FIGURE 2. Analytical model.

to the heat transfer from the phase interface with temperature $T_{F,SAT}$ to the coolant flow with temperature T_K with corresponding HTC k'. Two dots in HTC of condensing mixture $\ddot{\alpha}_G$ indicates that heat is transferred not only by conduction which is given by α_G but also by mass flow of condensing vapour, which is given by mass transfer coefficient β_G.

The heat flux between the gas-vapour mixture and the cooling water is determined by the heat and mass transfer resistances and the temperature difference of the fluids in the condenser.

$$\dot{q} = \ddot{\alpha}_G(T_{SAT} - T_{F,SAT})$$
$$= k'(T_{F,SAT} - T_K)$$
$$= k(T_{SAT} - T_K) \qquad (1)$$

The fundamental assumption in the model is that the condensate flows on a vertical wall in an annular film, similarly to the Nusselt condensation theory with HTC α_F. The vapour condenses on the film surface, while the gas accumulates near the phase interface. This forms another layer of non-condensable gas through which the vapour diffuses towards the phase interface. Heat flux, which is transferred from the gas-vapour mixture, can be divided into sensible heat given by HTC α_{cv} and latent heat given by α_c, as described by Equation (2). The mass transfer resistance occurs only in the mixture since the condensate film is formed only by water with a temperature at the wall $T_{W,F}$.

$$\dot{q} = \frac{1}{\dfrac{1}{\alpha_F} + \dfrac{1}{\alpha_{cv} + \alpha_c}}(T_{SAT} - T_{W,F}) \qquad (2)$$

The convective heat flow $\dot{q}_G$ transferred from the gas to the liquid film is calculated with respect to the mass transfer that occurs with heat transfer according to the Ackermann correction factor E_T (Equation (3)) with Equation (4) and Equation (5), where Φ_T is a non-dimensional mass flow, $\dot{n}$ local molar flux, $\tilde{c}_{pG}$ molar specific heat capacity and α_G convective HTC of the mixture.

$$\dot{q} = \alpha_G E_T(T_{SAT} - T_{F,SAT}) \qquad (3)$$

$$E_T = \frac{\Phi_T}{1 - \exp(-\Phi_T)} \qquad (4)$$

$$\Phi_T = \frac{\dot{n}\tilde{c}_{pG}}{\alpha_G} \qquad (5)$$

The latent heat corresponds to the vapour transferred through the gas layer to the phase interface. This can be determined by applying the heat and mass transfer analogy. Mass transfer is based on the same formal relation as heat transfer replacing the Nusselt number Nu with the Sherwood number Sh and the Prandtl number Pr with the Schmidt number Sc as shown in Equations (6) and (7). The relation between mass and heat transfer can then be described by the Lewis number Le according to Equation (8) with molar density of the gas n_G. The mass transfer coefficient is then applied to calculate the local condensing flow according to the diffusion of concentration (Equation (9)) where $\dot{r}_v$ is the relative molar flow of the vapour, $\tilde{y}_{v,F}$ is the molar concentration of vapour at the phase interface, $\tilde{y}_{v,B}$ is the molar concentration of vapour in the bulk mixture, and $\dot{n}_v$ is the local vapour molar flux.

$$Nu = CRe^{\alpha}Pr^{0.6} \qquad (6)$$

$$Sh = CRe^{\alpha}Sc^{0.6} \qquad (7)$$

$$\alpha_G = n_G\beta_G\tilde{c}_{pG}Le^{0.6} \qquad (8)$$

$$\dot{n} = n_G\beta_G \ln\left(\frac{\dot{r}_v - \tilde{y}_{v,F}}{\dot{r}_v - \tilde{y}_{v,B}}\right), \qquad (9)$$

where:

$$\dot{r}_v = \frac{\dot{n}_v}{\dot{n}}. \qquad (10)$$

During the calculation of the heat balance at certain parts of the condenser, it is necessary to know the condensation temperature of the vapour on the phase interface $T_{F,SAT}$. This temperature is calculated from Equation (10), including mass and energy balance. This equation is solved iteratively with the initial estimation of the film temperature at the phase
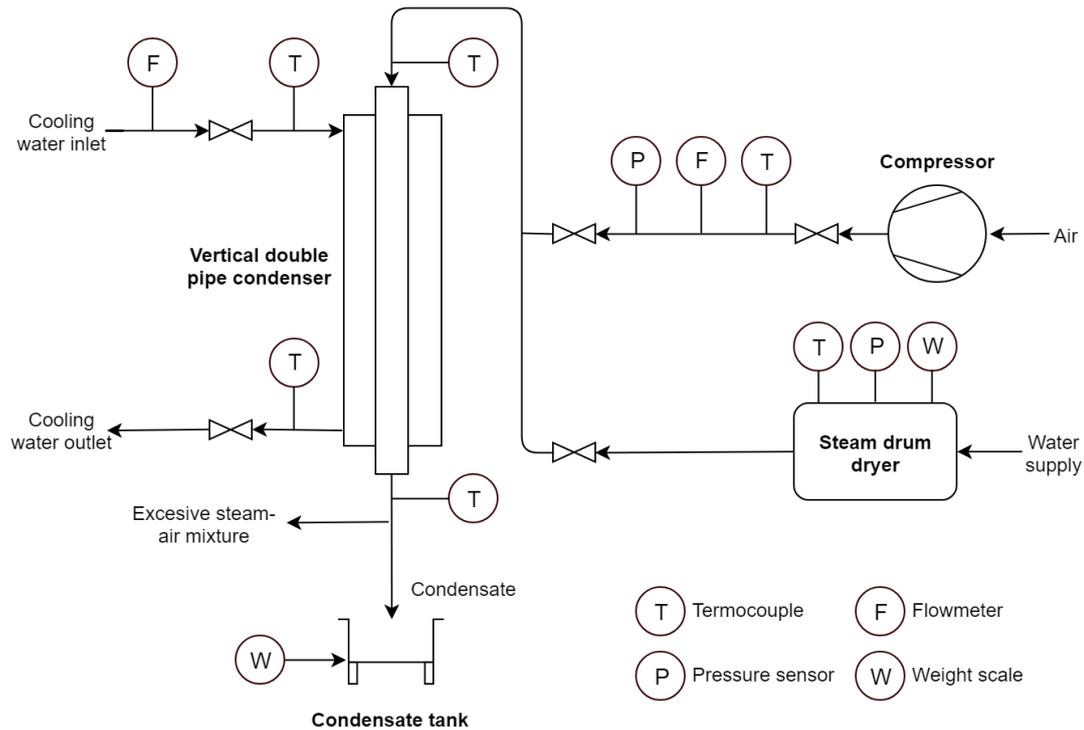
FIGURE 3. Schematic diagram of experimental setup.

interface with $\dot{N}_F$ being the film molar flux and T_F being the film temperature.

$$\dot{N}_F \tilde{c}_{pF} \frac{dT_F}{dA} + k'(T_{SAT} - T_{F,SAT}) = \dot{n}\Delta\tilde{h}_v$$
$$+ \alpha_G E_T (T_{SAT} - T_{F,SAT}) \quad (11)$$

Overall results are given by an arithmetic ratio of results from given segments. The overall condensation performance of the heat exchanger is calculated according to the steps shown below. Two parameters must be estimated at the beginning – the condensation temperature of the vapour on the film surface and the outlet temperature of the cooling water. The temperature of the film surface has to be estimated in each segment, while the temperature of the cooling water has to be estimated only in the outlet segment. The temperature of the cooling water at other points is given by the energy balance corresponding to the condensation and convection of the air-vapour mixture in the given segment. The HTC of the cooling water was experimentally determined by pure water vapour tests. The effects of the film flow mode, the shear stress of the flowing mixture, and the subcooling and superheating are included according to [14].

(1.) Input of initial values (mixture and cooling water inlet parameters – temperature, pressure, mass flow).

(2.) Estimation of the outlet temperature of cooling water.

(3.) Estimation of the saturation temperature at the phase interface of vapour.

(4.) Calculation of fluid thermodynamic properties according to [15].

(5.) Calculation of heat and mass transfer coefficients α_G; β_G.

(6.) Calculation of the local condensation rate and HTC of the film α_F.

(7.) Calculation of saturation temperature at the phase interface using the Ackermann correction factor.

(8.) Check if the calculated saturation temperature on the phase interface corresponds to the estimated (if not, back to step 3 – an adjustment of the saturation temperature on the phase interface is necessary).

(9.) Calculation of the condenser power, heat transfer coefficient, outlet cooling water temperature for a given segment.

(10.) Repeat the calculation from the beginning until the last segment is calculated.

(11.) Check if the calculated outlet temperature of the cooling water corresponds to the estimated temperature (if not, back to Step 2 – the adjustment of cooling water outlet temperature).

(12.) Results and average values.

3. EXPERIMENTAL APPARATUS

A schematic diagram of the experimental apparatus used for the theoretical model validation is shown in Figure 3. The system is designed as an open loop comprised of three parts: main test section; water

vapour and air supply section; cooling water section. The main test section comprises a vertical double-pipe heat exchanger made of two concentric stainless steel tubes. The mixture of water vapour and air enters the heat exchanger at the top and is directed vertically downwards through a calming section before flowing into the inner vertical tube. The cooling water flows upwards in the annulus. The heat exchanger is in counter-current configuration. The inner tube of the heat exchanger is 2000 mm long with an inner diameter of 23.7 mm and a wall thickness of 1.6 mm. The outer tube is 1500 mm long, with an inner diameter of 29.7 mm and a wall thickness of 2 mm. The tube material is stainless steel 1.4301 (AISI 304). The annulus created from these two concentric tubes is 1.6 mm in width. Stainless steel pins are used as spacers at three circumferential positions to keep the annulus concentric.

The steam generator was placed on the platform weight scale, which measured the amount of vapour generated. The generator produced steam steadily at a rate controlled by the power input to the electrical immersion heaters. In the first stage of the experiments, air was chosen as the NCG and blown in the mixing point by a compressor. The volume flow rate of air was measured by a rotameter. The pressure of the air was measured using a U-tube water manometer. The mixing chamber of water and air was designed so that any possible condensate occurring during the mixing of the vapour and air was flowing back to the steam generator. The flow rate of the cooling water was controlled by a regulating valve. Non-condensing gases in the water circuit were vented from the system through a manual gate valve at the exit of the condenser. Microfiber insulation and rubber foam were wrapped around the heat exchanger to prevent any potential heat loss. Four thermocouples were placed in condenser tapings measuring the inlet and outlet temperature of the cooling water and the inlet and outlet temperature of the water vapour-air mixture. All experiments were performed under atmospheric pressure. Measurements were conducted after the steady state of the system was reached.

4. RESULTS AND DISCUSSION

4.1. THEORETICAL ANALYSIS

The theoretical model was developed to predict the results from experimental measurements and analyse the condensation process. Six different air mass concentrations in the mixture were tested in the model, ranging from 23 % to 62 %. The condensation of the vapour – air mixture differs in several parameters as compared to condensation of pure vapour. As water vapour condenses along the condenser tube, the concentration of vapour in the mixture changes. Therefore, the HTC, the condensation rate, the saturation temperature, and most of the driving parameters change along the condense tube.
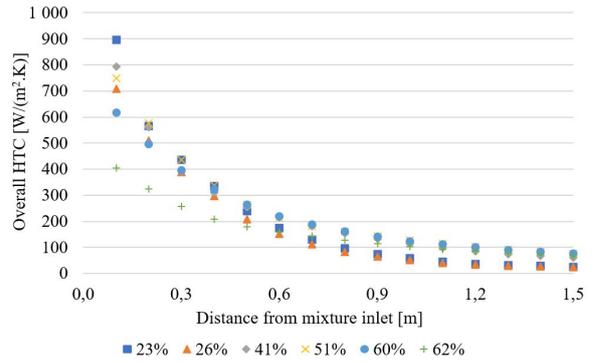

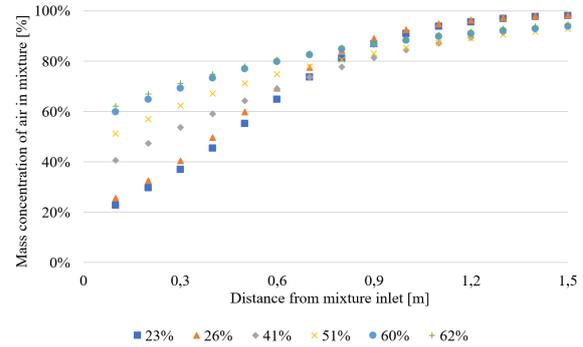FIGURE 4. Overall HTC along condenser length.

FIGURE 5. Air concentration in the mixture along condenser length.

The local HTC of the condenser along the tube length for all tests is shown in Figure 4. A rapid decrease in the HTC in the condenser inlet was calculated for the model for all cases of the condenser. As the vapour condenses along the condenser tube, several factors change, which leads to a reduction in vapour condensation and heat transfer; these factors are: increase of air concentration; decrease of velocity and Reynolds number of the mixture; increase of film thickness. As air concentration increases and the local condensation rate decreases, the overall HTC decreases rapidly in the condenser inlet. In the condenser outlet, HTC does not change so much since the local heat transfer is low and the amount of condensed vapour is also very small. Correspondingly, the HTC in the condenser outlet is very low because of the high concentration of air, which forms a gas layer next to the condensate film and prevents the vapour from reaching the phase interface. This can be seen in Figure 5, where the air concentration along the tube length is shown for all measurements. A strong increase in air concentration is observed at the beginning, and slow degradation is seen at the end as a result of a lower local condensation rate. The overall HTC of the condenser is determined by the heat resistance of certain parts of the condenser, as shown in Figure 2 and Equation (11), with the inner radius of the inner tube r_1, inner radius of the outer tube r_2, wall thermal conductivity λ_W, and HTC of the

			Tests					
			1	2	3	4	5	6
Air mass concentration	x	[-]	23 %	26 %	41 %	51 %	60 %	62 %
Air flow	$\dot{M}_a$	[kg/h]	0.58	0.58	1.37	2.04	2.63	2.04
Water vapour flow	$\dot{M}_p$	[kg/h]	1.97	1.68	2.01	1.94	1.77	1.24
Condensate flow	$\dot{M}_{KON}$	[kg/h]	1.98	1.68	1.87	1.58	1.16	-
Cooling water flow	$\dot{M}_K$	[kg/s]	0.0213	0.0213	0.0213	0.0165	0.0213	0.0281
Cooling water inlet temperature	T_{K1}	[°C]	14.8	14.8	14.7	15.0	14.6	16.0
Cooling water outlet temperature	T_{K2}	[°C]	32.0	29.2	30.8	30.4	25.8	22.2
Mixture inlet temperature	T_{p1}	[°C]	94.9	93.9	91.1	82.9	82.1	76.4
Mixture outlet temperature	T_{p2}	[°C]	43.6	40.6	74.6	66.5	64.6	61.3

TABLE 2. Measured values for all six tests.

cooling water $\propto_K$.

$$\frac{1}{r_1 k} = \frac{1}{r_1 \ddot{\propto}_G} + \frac{1}{r_1 \propto_F} + \frac{\ln \frac{r_2}{r_1}}{\lambda_W} + \frac{1}{r_2 \propto_K} \qquad (12)$$

Since the heat resistance of the cooling side and the tube wall of the condenser is quite low, the overall HTC is determined by the heat resistance of the condensing side. During the condensation of water vapour without non-condensing gases, the main heat resistance is usually formed by the condensate film on the cooling surface. This is quite well described by the Nusselt theory. In the case of the presence of NCG, the heat resistance is formed not only by the condensate film but also by the heat resistance of the mixture. The magnitude of heat resistance in the condensate film and the mixture depends on several parameters, mainly the concentration of air in the mixture, the flow of the condensate film, the flow of the mixture and the subcooling of the film. Due to the high amount of NCG in the mixture and low Re of the mixture, the heat resistance on the condensing side, in presented tests, was formed mainly by the heat resistance of the mixture. This can be seen in Figure 6 where the HTC of the film and the mixture are compared. The HTC of the condensate film is several times higher than the HTC of the mixture, therefore, the heat transfer is strongly affected by the heat and mass transfer in the gas-vapour mixture. Although the HTC of the film decreases along the condenser length as a result of the increase in film thickness, the HTC of the mixture is at least ten times lower and, in some cases, it is lower even more than two hundred times. This supports the claim that the HTC of the film can be neglected in some cases, since the overall HTC is formed mostly by the HTC of the mixture.

It can also be seen that it is quite difficult to fully condensate the vapour out of the mixture. Since the HTC decreases significantly at the end of the condenser, a very large condensation surface would be necessary to fully separate the vapour and the non-condensable gas. The initial gas concentration is not so crucial when the vapour must be fully condensed,
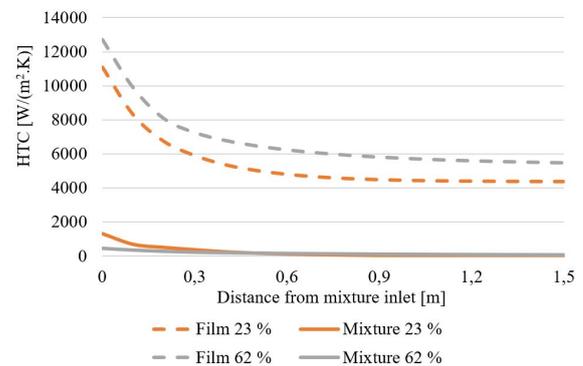

FIGURE 6. Comparison of HTC of film and gas – vapour mixture.

as the HTC is approaching similar parameters at the end of the condenser for all runs.

4.2. EXPERIMENTAL RESULTS

Experimental measurements with a mixture of water and air were conducted in the experimental loop with a vertical double-pipe condenser. The tests were carried out for six different air concentrations. The evaluation of experimental data was determined from the mass and energy conversion equations. The measured parameters and values are shown in Table 2.

The evaluation of the HTC for water vapour condensation is usually done according to the Nusselt's condensation theory. However, in the case when NCG is present, a deviation occurs between results from Nusselt's theory and experimental measurements. In Figure 7, a comparison between the results from experimental measurements and the results predicted with the Nusselt's theory for the mean HTC of the film is shown. As it can be seen, the Nusselt theory cannot be used by itself for a result prediction when NCG is present in the condensing mixture. Therefore, it might be useful to use one of the theoretical models presented in the previous section. In Figure 8, the measured amount of condensate captured during the tests is shown. With increasing air inlet concentration, the ratio of condensed vapour significantly
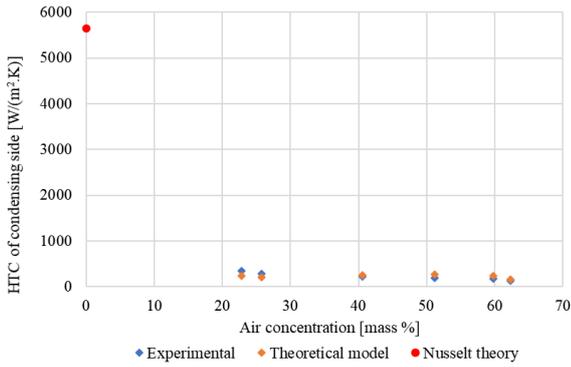
FIGURE 7. Condensing side HTC comparison obtained from the experiments, developed theoretical model and Nusselt theory.
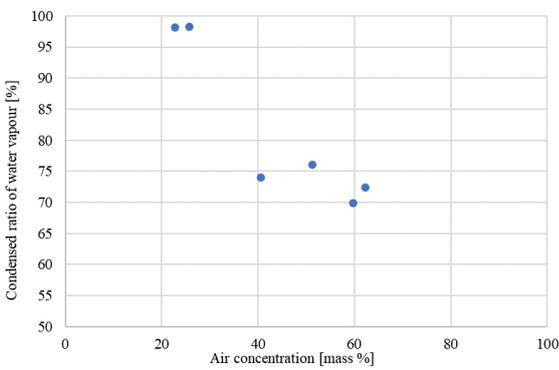

FIGURE 8. Dependence of the condensed vapour and the air concentration in the mixture.

decreases. It was observed that in the case of the inlet air mixture concentration of 20 %, almost all the vapour condensed. This is in accordance with the results from the theoretical model.

4.3. COMPARISON OF RESULTS FROM EXPERIMENTS AND THE THEORETICAL MODEL

The predicted results from the theoretical model were compared with the results from the experimental measurements. The results were compared with the overall condenser power and are shown in Figure 9. The heat rejected by the cooling water, determined by the experiments and calculated from the theoretical model, is in good agreement with the standard deviation within +25 % and −5 %. In the case of a lower NCG concentration, the theoretical model can predict, with a very high accuracy, the overall condenser power; however, at a higher NCG concentration, the model is less accurate. Another option to compare experimental and theoretical data is through the overall HTC, which is shown in Figure 7. The HTC predicted from the theoretical model for lower values of air inlet concentration are lower than those measured during the experiment. Although this might not be so accurate, since the overall HTC from the model is calculated as an arithmetic ratio of local values. Another reason
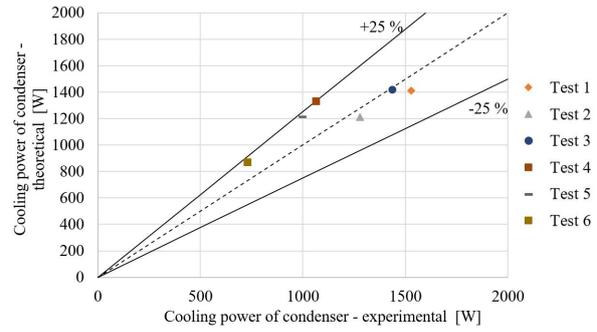

FIGURE 9. Comparison of condenser power of theoretical model and experiments.

why the HTCs from the theoretical model and experimental measurements differ might be the disturbance of the NCG layer by other phenomena. These might occur during condensation and were not considered in the presented model. In [16, 17], the suction effect, which occurs during the condensation of vapour in the presence of NCG, was analysed and it was concluded that it can improve HTC by even 20 %. The formation of mist can also improve HTC [18, 19]. This occurs when the mass transfer resistance in the mixture is much higher than the heat transfer resistance. However, the clear influence of the suction effect and the formation of mist on the HTC has not yet been determined. Therefore, including these phenomena in the model is rather difficult and unclear, even though it might be viable to do so, since it might improve the accuracy of the results predicted from the theoretical models.

5. CONCLUSIONS

Four theoretical methods for the determination of the HTC and heat transfer during condensation of vapour with gas are usually recommended in the literature: degradation and correlation factor, heat and mass transfer analogy, diffusion layer and boundary layer model.

For the theoretical model, based on heat and mass transfer analogy, it was observed that the overall HTC of the condenser decreases as the air concentration increases, also, as the Reynolds number of the mixture decreases, and/or the film thickness increases. An increase in air concentration has the strongest influence on the HTC. This is observed because of the mass transfer resistance of the vapour due to the layer of NCG near the phase interface. Increasing Re number of the mixture or disturbing this layer of NCG near the phase interface might, therefore, increase the HTC of the condensing mixture. The HTC of the film during the condensation of vapour in the presence of a high content of NCG can be several times higher than the HTC of the mixture. Neglecting the HTC of the film might not produce a significant error in calculation and can simplify the theoretical modelling. A significant decrease in film HTC is also seen at the beginning

of the condenser, which corresponds to local condensing flow. A rapid decrease in HTC is observed mainly in the condenser inlet, while in the condenser outlet, HTC is very low and does not change significantly. It was also observed that an effort to condensate all the vapour content out of the mixture leads to a much larger condensing surface, since the HTC is very low at the end of the condenser. Increasing the HTC in the condenser outlet can, therefore, rapidly increase the condenser power and might contribute to condensing a larger portion of the vapour out of the mixture.

An experimental measurement of water vapour condensation in the presence of high concentration of air was carried out in a counter-current vertical double-pipe condenser. Air mass concentration ranged between 23 % and 62 %. A significant decrease in the HTC on the condensing side can be seen in the model and experiment as compared to results from Nusselt theory. Therefore, using the Nusselt theory for vapour condensation in the presence of NCG is not suitable.

The results of the theoretical model and the experimental measurements were compared regarding the cooling power of the condenser. The results from the theoretical model and experiments are in good agreement with the standard deviation within $+25\,\%$ and $-5\,\%$. Therefore, the heat and mass transfer analogy might predict the power of the condenser and the HTC of vapour condensation in the presence of large amount of NCG with a sufficient accuracy. A larger accuracy is observed for a low NCG concentration than for a higher NCG concentration. Precaution is, therefore, recommended when using the model for a higher NCG concentration. Obtained results are valid for all vertical geometries when the width of the condensate film is negligible compared to the cross section of the flow. In addition, studying other factors that might influence the condensation of vapour in the presence of NCG, such as the suction effect and mist formation, can enhance the accuracy of the heat-mass transfer model. Experiments to determine the effect of NCG on water vapour condensation have been performed, so far, for an artificially prepared mixture of water vapour and air, also because of the availability of relevant literature references. Another goal of the research is to verify the process of water vapour condensation from a mixture with CO_2 to apply this method for drying flue gas from oxyfuel combustion.

List of symbols

a Air

A Heat exchanger area $[\mathrm{m}^2]$

C Geometric dimensionless number in empirical equation

$\tilde{c}_p$ Molar specific heat capacity $[\mathrm{J\,kg^{-1}\,K^{-1}}]$

E_T Ackermann factor $[-]$

$\Delta \tilde{h}_v$ Molar heat of condensation $[\mathrm{J\,mol^{-1}}]$

HTC   Heat transfer coefficient $[\mathrm{W\,m^{-2}\,K^{-1}}]$

k Overall heat transfer coefficient $[\mathrm{W\,m^{-2}\,K^{-1}}]$

k' Heat transfer coefficient between phase interface and coolant $[\mathrm{W\,m^{-2}\,K^{-1}}]$

K   Cooling water

Le Lewis number

n Molar density $[\mathrm{mol\,m^{-3}}]$

$\dot{n}$ Local molar flux $[\mathrm{mol\,m^{-2}\,s^{-1}}]$

$\dot{N}$ Molar flux $[\mathrm{mol\,s^{-1}}]$

NCG   Non-condensable gas

Nu Nusselt number $[-]$

p   Vapour

Pr Prandtl number

$\dot{q}$ Heat flux $[\mathrm{W\,m^{-2}}]$

r_1 Radius of inner tube $[\mathrm{m}]$

$\dot{r}_v$ Relative molar flow $[-]$

r_2 Radius of outer tube $[\mathrm{m}]$

Re Reynolds number $[-]$

Sc Schmidt number $[-]$

Sh Sherwood number $[-]$

$\tilde{y}$ Molar concentration $[-]$

Greek symbols

α Heat transfer coefficient $[\mathrm{W\,m^{-2}\,K^{-1}}]$

$\ddot{\alpha}_G$ Heat transfer coefficient of condensing side $[\mathrm{W\,m^{-2}\,K^{-1}}]$

β Mass transfer coefficient $[\mathrm{m\,s^{-1}}]$

λ Thermal conductivity $[\mathrm{W\,m^{-1}\,K^{-1}}]$

Φ_T Non-dimensional mass flow $[-]$

Subscripts

1   Inlet

2   Outlet

a   Power products in empirical equation

B   Bulk

c   Condensation

cv   Convection

F   Film

F,SAT   Film saturation

i   Inner

KON   Condensate

G   Gas

SAT   Saturation

v   Vapour

w   Wall

References

[1] O. Reynolds, H. E. Roscoe. I. On the condensation of a mixture of air and steam upon cold surfaces. *Proceedings of the Royal Society of London* **21**(139-147):274–281, 1873. https://doi.org/10.1098/rspl.1872.0056.

[2] M. Ge, S. Wang, J. Zhao, et al. Condensation of steam with high CO_2 concentration on a vertical plate. *Experimental Thermal and Fluid Science* **75**:147–155,

2016. https:
//doi.org/10.1016/j.expthermflusci.2016.02.008.

[3] J. Huang, J. Zhang, L. Wang. Review of vapor condensation heat and mass transfer in the presence of non-condensable gas. *Applied Thermal Engineering* **89**:469–484, 2015. https:
//doi.org/10.1016/j.applthermaleng.2015.06.040.

[4] J.-D. Li, M. Saraireh, G. Thorpe. Condensation of vapor in the presence of non-condensable gas in condensers. *International Journal of Heat and Mass Transfer* **54**(17-18):4078–4089, 2011. https:
//doi.org/10.1016/j.ijheatmasstransfer.2011.04.003.

[5] C. Chantana, S. Kumar. Experimental and theoretical investigation of air-steam condensation in a vertical tube at low inlet steam fractions. *Applied Thermal Engineering* **54**(2):399–412, 2013. https:
//doi.org/10.1016/j.applthermaleng.2013.02.024.

[6] W. Minkowycz, E. Sparrow. Condensation heat transfer in the presence of noncondensables, interfacial resistance, superheating, variable properties, and diffusion. *International Journal of Heat and Mass Transfer* **9**(10):1125–1144, 1966.
https://doi.org/10.1016/0017-9310(66)90035-4.

[7] F. Toman, P. Kracík, J. Pospíšil, M. Špiláček. Comparison of water vapour condensation in vertically oriented pipes of condensers with internal and external heat rejection. *Energy* **208**:118388, 2020.
https://doi.org/10.1016/j.energy.2020.118388.

[8] N. Maheshwari, D. Saha, R. Sinha, M. Aritomi. Investigation on condensation in presence of a noncondensable gas for a wide range of reynolds number. *Nuclear Engineering and Design* **227**(2):219–238, 2004.
https://doi.org/10.1016/j.nucengdes.2003.10.003.

[9] H. C. No, H. S. Park. Non-iterative condensation modeling for steam condensation with non-condensable gas in a vertical tube. *International Journal of Heat and Mass Transfer* **45**(4):845–854, 2002.
https://doi.org/10.1016/S0017-9310(01)00176-4.

[10] P. Kracík, F. Toman, J. Pospíšil. Effect of the flow velocity of gas on liquid film flow in a vertical tube. *Chemical Engineering Transactions* **81**:811–816, 2020.
https://doi.org/10.3303/CET2081136.

[11] S. Kuhn, V. Schrock, P. Peterson. An investigation of condensation from steam–gas mixtures flowing downward inside a vertical tube. *Nuclear Engineering and Design* **177**(1-3):53–69, 1997.
https://doi.org/10.1016/S0029-5493(97)00185-4.

[12] W. Nusselt. *Des oberflachenkondensation des wasserdamfes*, vol. 60. Z. VereinesDeutsch. Ing., 1916.

[13] K. Karkoszka. *Theoretical investigation of water vapour condensation in presence of noncondensable gases*. Licentiate thesis, Royal Institute of Technology, Division of Nuclear Reactor Technology, Stockholm, Sweden, 2005.

[14] VDI e. V. *VDI Heat Atlas*. Springer Berlin, Heidelberg, 2010. https://doi.org/10.1007/978-3-540-77877-6.

[15] A. P. Colburn, O. A. Hougen. Design of cooler condensers for mixtures of vapors with noncondensing gases. *Industrial & Engineering Chemistry* **26**(11):1178–1182, 1934. https://doi.org/10.1021/ie50299a011.

[16] L. E. Herranz, A. Campo. Adequacy of the heat-mass transfer analogy to simulate containment atmospheric cooling in the new generation of advanced nuclear reactors: Experimental confirmation. *Nuclear Technology* **139**(3):221–232, 2002.
https://doi.org/10.13182/NT02-A3315.

[17] S. Oh, S. T. Revankar. Experimental and theoretical investigation of film condensation with noncondensable gas. *International Journal of Heat and Mass Transfer* **49**(15-16):2523–2534, 2006. https:
//doi.org/10.1016/j.ijheatmasstransfer.2006.01.021.

[18] M. Y. a Hijikata Kunio. Free convective condensation heat transfer with noncondensable gas on a vertical surface. *International Journal of Heat and Mass Transfer* **16**(12):2229–2240, 1973.
https://doi.org/10.1016/0017-9310(73)90009-4.

[19] H. C. Kang, M. H. Kim. Characteristics of film condensation of supersaturated steam–air mixture on a flat plate. *International Journal of Multiphase Flow* **25**(8):1601–1618, 1999.
https://doi.org/10.1016/S0301-9322(98)00077-9.